A significance of L-shaped geosynthetic drain (LGD) against seepage flow

Hara, K.
TaiyoKogyo Corporation(Sun), Japan

Shibuya, S., Saito, M., Torii, N., Chae, J.
Kobe University, Japan

Masuo, T.
TaiyoKogyo Corporation(Sun), Japan

Keywords: unsaturated soil, embankment, numerical analysis, full-scale test, geosynthetics

ABSTRACT: Shibuya et al (2008) has proposed a remedial method to protect embankment from the invasion of seepage flow by using L-shaped geosynthetic drains (LGD). In this paper, the behavior of a large-scale test wall (4m long x 2m wide and 2.5m high) was examined when the water seepage was initiated from the back of the test fill. Three test cases were carried out; i.e., no geosynthetic drains installed, layered geosynthetic drains mounted horizontally (conventional method), and L-shaped geosynthetic drain. In all of these cases, the full-scale embankment with weathered granite soil was fully instrumented using suction probes, moisture sensors and inclinometers to measure the lateral deformation of the embankment. The performance of the test fill was interpreted by comparing the test result against the result of numerical analysis. The design of the LGD is also discussed based on the results of numerical analysis. It is manifested that the horizontally arranged drains are not effective in preventing the water flow into the embankment, whereas the LGD is the most effective in mitigating the embankment failure.

1 INTRODUCTION

A failure of Terre Armée wall reported recently by Shibuya et al. (2007) was induced by seepage water flow in the event of heavy rainfall, which in turn weakened the initially unsaturated fill material and also pushed the wall by the accumulated water pressure behind the wall. Based on this experience, the use of an L-shaped geosynthetic drain (LGD) comprising a set of vertical and horizontal planar-geosynthetics has been proposed by Shibuya et al (2008). Saito et al (2008) has performed numerical simulation in which the efficiency of the LGD system in preventing seepage water flow into the fill was successfully demonstrated.

In this paper, the effectiveness of LGD in preventing the seepage flow into the embankment is demonstrated in a series of numerical analysis, in which the result with LGD was compared to the case comprising horizontally layered geosynthetic drain system. A full-scale seepage flow test using an embankment (3.9m in length, 2.0m in width and 2.5m in height) made of a well-graded decomposed granite soil was carried out. The behavior of the test embankment undertaking seepage flow from the back was carefully examined by monitoring vertical settlement, lateral deformation, pore pressures and moisture content at several points in the test embankment.

2 NUMERICAL SIMULATION

2.1 *Governing equation and boundary conditions*

In the seepage analysis, the following Richards' equation (Richards 1931) is employed as the governing equation;

$$\left(C+\beta S_s\right)\frac{\partial \psi}{\partial t}=\nabla\cdot\left[\mathbf{K}\cdot\left(\nabla\psi+\nabla Z\right)\right] \tag{1}$$

where C is the specific water capacity (= ϕdS_w/dψ) (n.b., ϕ : porosity, and S_w : the degree of saturation ($0\leq S_w\leq 1$)), S_s is the specific storage coefficient, K is the hydraulic conductivity tensor, ψ is the pressure head, and Z is the elevation head. Note that β is equal to unity in the saturated zone involved with $S_w = 1$, and to zero in the unsaturated zone with $S_w \neq 1$. The K can be expressed in terms of the relative permeability k_r and the saturated hydraulic conductivity Ks, i.e.,

$$\mathrm{K} = k_r \cdot \mathrm{Ks} \tag{2}$$

The boundary condition on Γ_1, where the pore pressure head is defined, is given by

$$\psi = \psi_1 \ \ on \ \ \Gamma_1 \tag{3}$$

On the boundary Γ_2, the flux q is defined in the following form;

$$q = q_2 = -\mathbf{n}\cdot\mathbf{K}\cdot(\nabla\psi + \nabla Z) \quad on \quad \Gamma_2 \tag{4}$$

where **n** denotes the outwardly directed unit normal vector.

The relative permeability k_r is an essential parameter in the seepage analysis. This property is considered as a function of S_w, whereas the S_w is considered as a function of capillary pressure ψ_c ($\equiv -\psi$). Among many mathematical models previously proposed to describe the water retention curve, the van Genuchten equation (van Genuchten 1980) (i.e., VG model) is employed in the present study; i.e.,

$$S_e = \frac{S_w - S_r}{S_f - S_r} = \left\{1 + (\alpha\psi_c)^n\right\}^{-m} \tag{5}$$

where S_e is the effective saturation, S_r is the residual saturation, S_f is the saturation at $\psi_c = 0$, and α, n and m are parameters. The parameters, n and m, are both dimensionless, whereas α has the dimension that can be defined as the reciprocal of the pressure head. The parameters n and m are not independent to each other, and they are related by

$$m = 1 - 1/n \tag{6}$$

The relative permeability and effective saturation are interrelated as shown in the following form (Maulem 1976) ;

$$k_r = S_e^{\varepsilon}\left\{1 - \left(1 - S_e^{1/m}\right)^m\right\}^2 \tag{7}$$

where ε is a parameter regarding the degree of interconnection among voids. Generally, a value of 0.5 is used for ε. The water retention curve and relative permeability can be calculated when the parameters α, n, S_r and S_f are all given. More details regarding the numerical techniques are given by Saito et al (2008).

2.2 *Effectiveness of LGD*

Figure 1 shows three cases for which the seepage flow was simulated. The idealized flow domain was assumed in a manner that impervious boundary was considered at the bottom, the flux $q = 0$ at the seepage surface boundary at the right-hand vertical wall when $\psi < 0$, and $\psi = 0$ when $q < 0$. The left-hand vertical plane is the boundary to generate the water pressure varying with time. It was postulated that the water pressure rose linearly with time to reach the maximum value corresponding to H = 0.9m. The S_w prior to seepage flow was set 0.46. In the first case, no geo-drain was employed in the model ground having the $k_s = 2.3\times10^{-3}$cm/s, the length of 2m and the height of 1.0m (see Fig.1a). In the second case, a series of geosynthetic drain was employed to form horizontal layers (see Fig.1b). The permeability of the geosynthetic drain was assumed k_d = 1.0cm/s and k_d = 10cm/s. The LGD was employed in the third case (see Fig.1c).

Figure 2 shows the distribution of degree of saturation at steady flow state. It is obvious in that the LGD is effective in preventing seepage water flow into the protected region. The effect is more significant when the permeability of geosynthetic drain is large. Note also that the horizontally layered geodrain system is less efficient compared to the LGD system in terms of reducing the area of saturation.

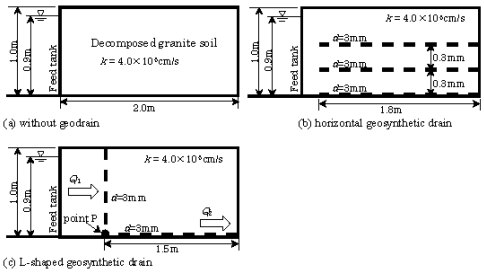

Figure 1. Cases of numerical simulation performed.

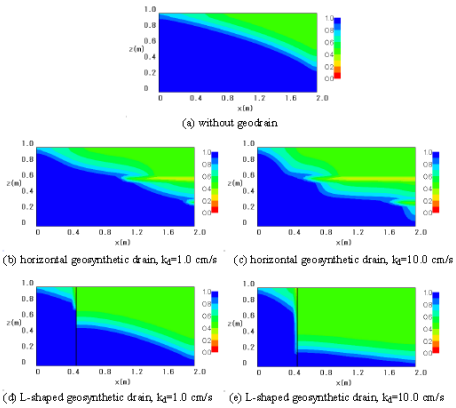

Figure 2. Results of numerical simulation.

3 EXPERIMENT

3.1 *A large-scale embankment*

The test embankment was made by using approximately 20m^3 of decomposed granite soil having the mean particle diameter of 1.15mm, and the maximum dry density of 1.938g/cm^3 involved with the optimum water content of 11.6% (for details, see Saito et al 2008). The embankment was constructed at stages, each in which the prescribed amount of the air-dried soil having the initial water content of 8% on average was compacted to form a 0.25m thick layer.

A couple of comparative tests without geodrain, with horizontal geosynthetic drain and with the LGD, i.e., case 1, case 2, and case 3, respectively, were performed. Figures 3 and 4 show the configuration of these three embankments. The dry density was

about 85%, about 86% and nearly 90% of the maximum dry density for case 1, case 2 and case 3, respectively. It should be mentioned that in case 3 embankment with LGD, the compaction of the upstream portion facing the water supply pipes was not easy owing to the limited working space so that the degree of compaction was about 86%, which was lower than the downstream portion with the compaction of nearly 90%.

In these tests, the seepage flow was initiated by raising the water level in the water supply pipes installed at one end of the embankment. The other end was reinforced by using five rectangular-shaped EPS blocks, each wrapped with a sheet of geogrid. It should be mentioned that the EPS blocks were light in weight, and not connected to each other. Accordingly, the wall facing was rather considered flexible. In case 3 embankment, a set of geosynthetic sheets comprising a 11mm thick core material covered with non-woven geotextiles jacket was installed vertically and horizontally to form the LGD system.

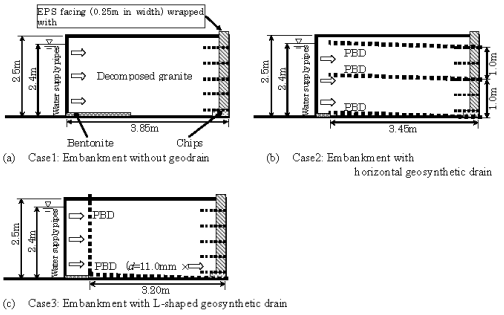

Figure 3. Configuration of test embankments.

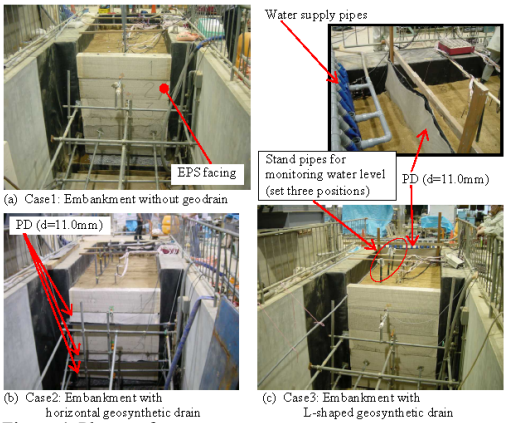

Figure 4. Photos of test embankments.

Figure 5, for example, shows instrumentations used for monitoring the behavior of the embankment of case 3. The deformation was measured with the settlement plates and the inclinometers for the vertical and horizontal deformation, respectively. An inclinometer made of a PVC pipe was fixed at the bottom. It comprised a set of strain gauges mounted every 0.25m along the vertical to measure the deflection of the pipe. The seepage water level in the embankment was continuously monitored at three positions by using stand pipes.

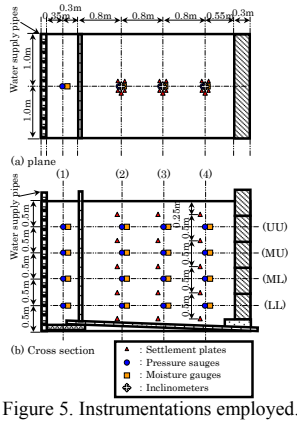

Figure 5. Instrumentations employed.

3.2 *Seepage flow test*

The upstream water level was raised quickly to reach a level of 2.4m from the bottom (see Fig3). In case 3 with LGD, the filling and de-watering cycle was repeated. Figure 6 shows the idealized flow domain in case 3 test. Following the (x, z) co-ordinate in Fig.6, impervious boundaries involved with $q = 0$ are considered at $z = 0$m and $z = 2.5$m at the bottom and surface of the embankment, respectively. As for seepage surface at $x = 3.6$m, the condition with $q = 0$ is satisfied when the pressure head $\psi < 0$, and $\psi = 0$ when $q < 0$.

The upstream vertical plane at $x = 0$m is the boundary to generate the water pressure varying with time. It was postulated that the water pressure rose linearly with time to reach the maximum value of $H = 2.4$m. Conversely, it was assumed that in the event of dewatering, the H reduced by satisfying;

$$\frac{dH}{dt} = -\frac{Q_i(t,H)}{A} \tag{8}$$

where A represents the cross-section area of the water tank, and Q_i denotes the rate of water inflow into the test embankment. The Q_i was not a priori given so that it was calculated by iteration.

The permeability of geosynthetic drain was assumed 5.0 cm/sec. The permeability soil used in the analysis are shown in Table 1. Porosity ϕ was fixed at the measured value of 0.35, implying that no volume change took place throughout the seepage test.

An example for the relationship between capillary pressure and the degree of saturation is shown in Fig.7, in which the response at UU-1 in case 1 test is shown, together with the result of numerical simula-

tion by means of the VG model (van Genuchten 1980).

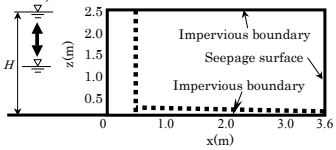

Figure 6. Flow domain assumed in the numerical analysis.

Table 1. Permeability of decomposed granite soil

Item	Permeability
Measured	5.3×10^{-4} cm/sec
Simulation	
Case 1	8.5×10^{-3} cm/sec
Case 2	7.0×10^{-3} cm/sec
Case 3	
- upstream	2.3×10^{-3} cm/sec
- downstream	6.0×10^{-4} cm/sec

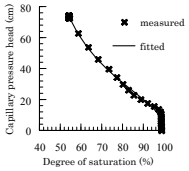

Figure 7. Water retention curve for case 1. (observation vs simulation)

4 DISCUSSIONS

4.1 *Seepage flow characteristics*

The variation of degree of saturation with time is examined in Fig.8, in which the response at LL-1 and LL-4 in case 1 is examined (see Fig.5). Figure 9 shows similar observations for the variation of pore pressure head with time. The contours of ψ since the commencement of water filling are shown in Fig.10, in which the measured water level in the standing pipes are also plotted for comparison. Note that the numerical analysis is capable of simulating well the variations of pore pressure as well as the degree of saturation with time.

Comparisons between the observation and the numerical simulation for case 3 test are made in Figs.11 and 12, in which the variation of S_w with time at UU1 and LL-3 (see Fig.5) as well as the rate of discharge are examined, respectively. Similar to case 1, the numerical analysis was good enough for simulating not only the variations of pore pressure and the degree of saturation with time but also the rate of discharge.

Figure 13 shows the contours of S_w at the elapsed time t=140hrs in case 3 test, which corresponds to a steady flow at the second stage of water filling (see Fig.12). It is obvious in this figure that the LGD is highly effective in reducing the downstream water level behind the vertical drain.

In case 2 test, the numerical simulation was not remarkably good, since the flow curve was disturbed by the horizontal geosynthetics having small holes for instrumentations.

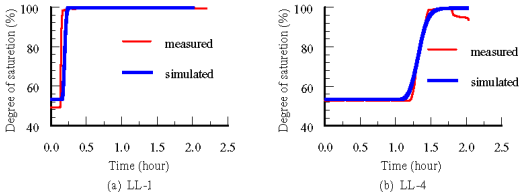

Figure 8. Variation of S_w with time. (case 1)

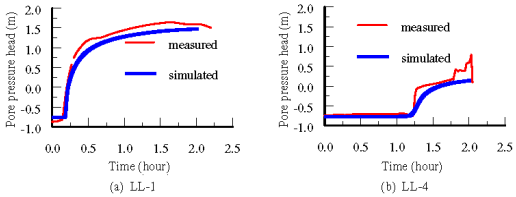

Figure 9. Variation of ψ with time. (case 1)

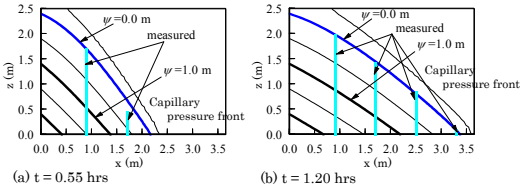

Figure 10. Contours of ψ. (case 1)

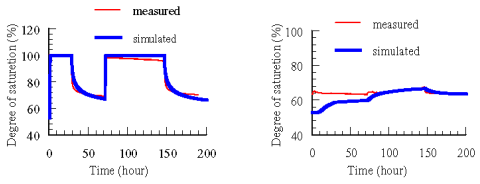

Figure 11. Variation of S_w with time. (case 3 with LGD)

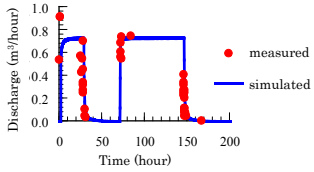

Figure 12. Discharge with time. (case 3)

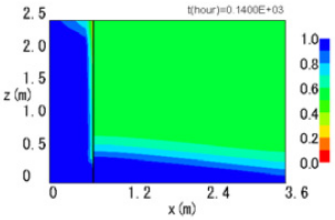

Figure 13. Simulation of S_w at t=140 hrs. (case 3)

4.2 *Deformation of test embankment*

In case 1 embankment without the geosynthetic drain, the embankment failed after about 80mins since the start of water filling. The failure occurred as soon as the seepage front reached to the chips mounted underneath the EPS block wall. As seen in Fig.14, a tension crack developed parallel to the wall at a distance of about 50cm away from the edge of the EPS wall. The failure may well be triggered by the compression failure of soil adjacent to the EPS block facing. Note also that the EPS wall reinforced with short geogrid was still effective in preventing collapse of the wall facing.

The variation of horizontal deformation with time in case 1 embankment, together with the contours of pore pressure head is shown in Fig.15. On water filling, the upstream soil at the surface deformed by about 13mm towards the wall, whereas the other part of the embankment exhibited no deformation at all (refer to the instant at t=10min). As the seepage flow gradually progressed towards the wall, the deformation also propagated towards the downstream possibly due to the increase in water pressure behind the embankment at $x = 0$m. At 78mins after the filling (i.e., a few minutes before the collapse), the wall was pushed away by about 12mm at the middle and upper measuring points. The amount of displacement of the wall virtually coincided with those of three inclinometers at the corresponding level, which in turn suggests no resistance of the wall against the earth pressure. Conversely, the need for a rigid facing is strongly suggested in order to resist against the increase in earth pressure induced by the water pressure at the other end of the embankment.

In case 2 embankment with horizontal geosynthetic drain, tension cracks were observed on the surface (Fig.16). Moreover, the discharge of water from the tip of the geosynthetic drain was a little.

The response of horizontal deformation in case 2 embankment, together with the contours of pore pressure head is shown in Fig.17, inplying that the speed of water level rise in case 2 embankment was slower as compared with case 1.

Although the wall facing of case 2 embankment was significantly deformed in the horizontal direction, involved with the maximum deformation of 38.8mm, the case 2 embankment did not collapse. It is considered that the horizontal geosynthetic drain acted as a tensile reinforcement in the embankment. It is suggested that the degree of saturation in the embankment was nearly 100%, despite that it was not observed rise of the water level beside the wall facing (i.e., downstream).

In case 3 embankment with LGD, the embankment showed no sign of large deformation as examined over a period of one week. As stated earlier, the LGD was effective in reducing the downstream water level. As it can be seen in Fig.12, the water discharged as much as 0.7m^3 per hour from the tip of the bottom geosynthetic drain. Figure 18 shows the discharge of water from the tip of geosynthetic drain.

The response of horizontal deformation in case 3 embankment, together with the contours of pore pressure head is shown in Fig.19. A trend was obvious for the horizontal deformation that the embankment deformed towards the wall and away from the wall in a synchronized manner with the filling and dewatering, respectively. However, the amount of the overall deformation was insignificant as compared to the case 1. The efficiency of the LGD in reducing significantly the deformation of the protected region of the embankment is well demonstrated in these tests.

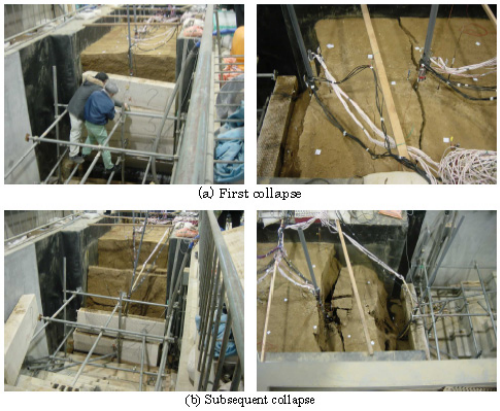

Figure 14. Collapse of case 1 embankment.

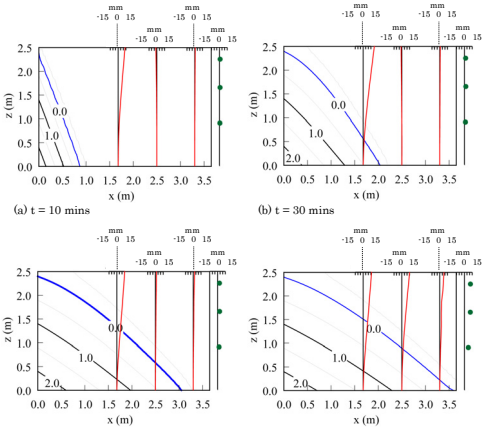

Figure 15. Horizontal deformation with contours of pore pressure head. (case 1)

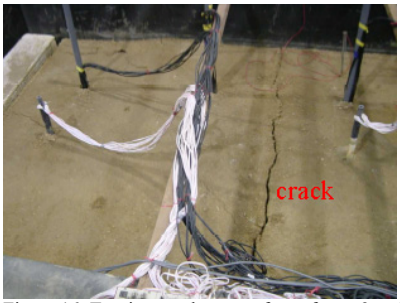

Figure 16. Tension cracks on surface of case 2 embankment.

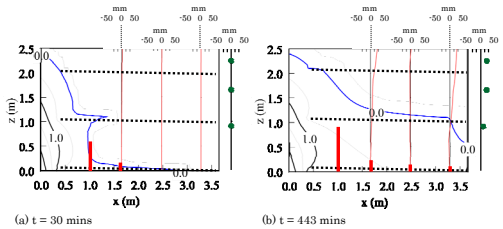

Figure 17. Horizontal deformation with contours of pore pressure head. (case 2)


Figure 18. Discharge of water from the tip of geosynthetic drain. (case 3)

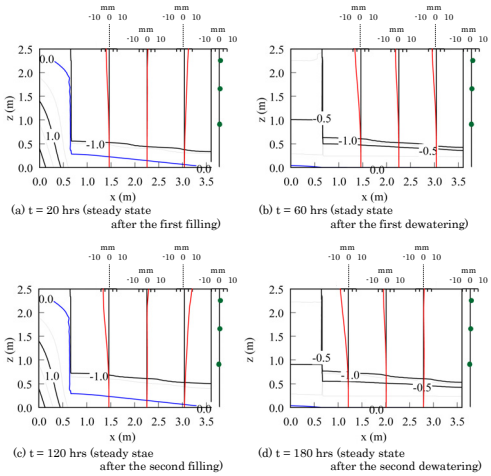

Figure 19. Horizontal deformation with contours of pore pressure head. (case 3)

5 CONCLUSIONS

The LGD is effective in preventing seepage water flow into the enbankment. The effect is more significant when the permeability of geosynthetic drain is large. The horizontally layered geo-drain system is less efficient compared to the LGD system in terms of reducing the area of saturation in the embankment. It was successfully demonstrated in the seepage flow test that the LGD was effective in reducing significantly the water level as well as the soil deformation of the protected zone against the attack of seepage flow from the back. It was also manifested that the numerical analysis is capable of simulating many aspects of the seepage characteristics such as the variations of soil suction and capillary pressure with time. When the L-shaped geosynthetic drain LGD was not employed, the test embankment failed as soon as the seepage flow reached to the wall. Therefore, the need for a rigid facing, together with the LGD is strongly suggested.

ACKNOWLEDGEMENT

The research was supported by research grant-in-aid No. 19360214 from the Ministry of Education and Science in Japan.

REFERENCES

Luckner, L., van Genuchtn, M.Th. & Nielsen, D.R. 1989. A Consistent Set of Parametric Models for the Subsurface, *Water Resources Research*, *Vol.25*, pp.2187-2193.

Maulem, Y. 1976. A new model for predicting the hydraulic conductivity of unsaturated porous media, *Water Resources Research*, *Vol.12*, pp.513-522.

Richards, L. A. 1931. Capillary Conduction of Liquids through Porous Mediums, *Physics*, *1*, pp.318-333.

Saito, M., Shibuya, S., Mitsui, J. & Hara, K. 2008. L-shaped geodrain in embankment -model test and numerical simulation-, *Proceedings of the 4th Asian Regional Conference on Geosynthetics*, *Shanhai*, pp.428-433.

Scott, P. S., Farquhar, G. J. & Kouwen, N. 1983. Hysteretic Effects on Net Infiltration, *In Advances in Infiltration*, *Am. Soc. Agric. Eng.*, *St. Joseph*, *MI*, pp.163-170.

Shibuya, S., Kawaguchi, T. & Chae, J.G. 2007. Failure of Reinforced Earth as Attacked by Typhoon No.23 in 2004, *Soils and Foundations*, *47-1*, pp.153-160.

Shibuya, S., Saito, M., Hara, K. & Masuo, T. 2008. Watertight embankment using L-shaped geosynthetic drain -Model test and numerical simulation-, *Geosynthetics Engineering Journal*, *Vol.23*, *Japan Chapter of International Geosynthetics Society*, pp.139-146.

van Genuchten, M. T. 1980. A closed-form equation for predicting the hydraulic conductivity of unsaturated soils, *Soil Science Society American Journal*, *Vol.44*, pp.892-898.